Drug Design, Development and Therapy

Dovepress

open access to scientific and medical research

Open Access Full Text Article

ORIGINAL RESEARCH

Dual-Drug Nanosystem: Etoposide Prodrug and Cisplatin Coloaded Nanostructured Lipid Carriers for Lung Cancer Therapy

Min Du[1], Jianbo Yin[2]

[1]Department of Pharmacy, Affiliated Hospital of Jiangnan University, Wuxi, Jiangsu Province, 214000, People's Republic of China; [2]Department of Pharmacy, Wuxi Dashan Medical Beauty Clinic, Wuxi, Jiangsu Province, 214001, People's Republic of China

Correspondence: Jianbo Yin, Email yinjianbodmbc@outlook.com

Purpose: Cisplatin (CDDP) and etoposide (Etp) are recommended first-line therapy for lung cancer. Nanostructured lipid carriers (NLCs) are engineered to deliver drugs for lung cancer treatment. In the present study, NLCs were applied to coload an Etp prodrug (EtpP) and CDDP.

Methods: The Etp prodrug was synthesized by linking the phenolic hydroxyl group of Etp with polyethylene glycol (PEG). EtpP and CDDP coencapsulated NLCs (EtpP–CDDP NLCs) were prepared using film ultrasound. Cytotoxicity of drugs and drug-containing NLCs was assessed by evaluating cell viability using MTT assays. In vivo antitumor efficiency of EtpP–CDDP NLCs was evaluated on lung cancer–bearing xenografts.

Results: EtpP–CDDP NLCs showed a uniformly spherical morphology with a size of 176.8±4.9 nm and ζ-potential of –31.9±3.2 mV. Cellular uptake efficiency of EtpP–CDDP NLCs was 57.4%±3.9% on A549/DDP cells. EtpP–CDDP NLCs exhibited more sustained plasma retention, the highest drug distribution in tumors, and the highest tumor-inhibition rates in lung tumor–bearing mice.

Conclusion: EtpP–CDDP NLCs improved tumor-cell uptake, cytotoxicity, and tumor-inhibition efficiency, and could be used as a promising drug-delivery system for lung cancer combination therapy.

Keywords: lung cancer, prodrug, etoposide, cisplatin, nanostructured lipid carriers

Introduction

Lung cancer is the leading cause of cancer death in developed countries, and can be divided into two major classes: non–small cell lung cancer (NSCLC; about 85%) and small-cell lung cancer (about 15%).[1–3] Patients with NSCLC have low overall relative 5-year survival: 25% in the US from 2009 to 2015.[4] On the basis of clinical studies, the National Comprehensive Cancer Network NSCLC Panel recommends cisplatin (CDDP) combined with docetaxel, etoposide (Etp), gemcitabine, or vinorelbine for preoperative and postoperative chemotherapy.[5–7] Arriagada et al found that CDDP plus Etp in patients with completely resected NSCLC improved patient survival by 56.5%.[5] Senan et al used Etp 50 mg/m^2 and CDDP 50 mg/m^{2}intravenously on patients with stage IIIA/B unresectable nonsquamous NSCLC randomly.[7] Unfortunately, these nonselective combination chemotherapies with multidrug resistance hindered clinical application. Therefore, major efforts have focused on the development of targeted drug-delivery systems based on prodrugs, nanocarriers, and ligand-modified nanoparticles.

CDDP combined with Etp is recommended first-line therapy for NSCLC.[5] CDDP is a cytotoxic antitumor drug. Its main mechanism involves the binding of genomic DNA in the cell nucleus and interfering with transcription to lead to cell death.[8] Its main side effects are nephrotoxicity and peripheral neuropathy. Recently, studies reported that targeted nanocarriers could enhance CDDP's efficacy and reduce its toxicity in healthy cells.[9,10]

The topoisomerase II inhibitor Etp inhibits DNA production by affecting the premitotic phase of cell division.[11] Poor solubility and chemical instability are major limits to its clinical application.[12] A prodrug is a kind of compound containing a parent drug that carries out biotransformation in vivo through chemical or enzymatic cleavage, and can

Received: 20 August 2022
Accepted: 12 November 2022
Published: 5 December 2022

effectively transfer active molecules.[13] Prodrug approaches have been developed to modify solubility, increase therapeutic efficacy, and reduce toxicity.[14] Schmidt et al synthesized a glucuronide-based prodrug of Etp that exhibited less cytotoxicity and more water-solubility than Etp itself.[15] In this study, we designed a novel amphiphilic Etp prodrug and tested it on a hydrophobic group (Etp group) and a hydrophilic group (polyethylene glycol, PEG).

Nanoparticles have a length of about 1–100 nm.[16] Nanoparticles are attractive for drug delivery because they have important and unique characteristics, such as much larger surface area:mass ratio than other particles, quantum properties, and the ability to adsorb and carry other compounds.[17] Nanoparticles have been exploited to enhance the pharmacokinetic properties and therapeutic effects of drugs.[18] Lipid nanoparticles are colloidal particles composed of biocompatible and biodegradable lipid matrices, among which nanostructured lipid carriers (NLCs) constituted of blends of lipids in solid and liquid state can be considered the latest generation.[19] NLCs have been engineered to deliver drugs for lung cancer treatment.[20,21] In the present study, NLCs were applied to coload an Etp prodrug (EtpP) and CDDP. EtpP and CDDP coencapsulated in NLCs (EtpP–CDDP NLCs) were prepared and characterized. The in vitro and in vivo antitumor efficiency of EtpP–CDDP NLCs was evaluated and compared with Etp and/or CDDP-loaded NLCs.

Methods

Materials

Etp, CDDP, oleic acid, glyceryl monostearate, coumarin 6 (C_6), and MTT were purchased from Sigma Aldrich (St. Louis, MO). Polyethylene glycol (PEG-NH_2) was purchased from Xi'an Ruixi Biological Technology (Xi'an, China). Other chemicals were of analytical grade or high-performance liquid chromatography grade and used without further purification.

Cells and Animals

Bronchial epithelium transformed with Ad12-SV40 2B (BEAS-2B cells), human lung cancer cells (A549 cells), and human umbilical vein endothelial cells (HUVECs) were obtained from the American Type Culture Collection (Manassas, VA). A CDDP-resistant human lung cancer cell line (A549/DDP) was produced by Yiyan Biotechnology (Shanghai, China). Female BALB/c mice derived nu/nu (18–22 g) were purchased from Vital River Laboratory Animal Technology (Beijing, China). A549/DDP cells (10^6) were injected subcutaneously in the dorsal skin of BALB/c mice. The tumors were grown to around 100 mm^3 to obtain mice bearing A549/DDP cell xenografts. All animal experiments were approved by the Animal Ethics Committee of Wuxi Dashan Medical Beauty Clinic and followed the policies of the National Institutes of Health *Guide for the Care and Use of Laboratory Animals*.

Synthesis of Etp Prodrug

EtpP was synthesized by linking the phenolic hydroxyl group of Etp with PEG (Figure 1).[22] In brief, PEG-NH_2 (1 equivalent) and phosgene (1.5 equivalents) were dissolved in CH_2Cl_2 (10 mL) at 0°C, then triethylamine (TEA, 3 equivalents) was added dropwise to get PEG-NH-COCl. DMAP (1.2 equivalents) was added to PEG-NH-COCl, followed by adding Etp (1.2 equivalents) in CH_2Cl_2 (10 mL). The mixture was stirred (60 min) and the solvent removed under reduced pressure. The product was purified by column chromatography on silica gel (CH_2Cl_2/CH_3CN: 8/2). A white solid (77%) was isolated to achieve EtpPEG (EtpP). ^{1}H NMR of EtpPEG in dimethyl sulfoxide-d_6 at 300 MHz: δ 8.21 and 7.38 (–NH–C(=O)–), 6.72–6.01 (belonging to Etp), 4.12 (–O–CH_2–C(=O)–N–), 3.59–3.81 (belonging to PEG), 1.95 (3, –CH_2–C(=O)–N–), 1.26 (–CH_2–), 0.96 (–CH_3).

Preparation of EtpP–CDDP NLCs

EtpP–CDDP NLCs were prepared using film ultrasound.[23] Briefly, an oil phase was formed by dissolving EtpP (20 mg), CDDP (10 mg), oleic acid (90 mg), and glyceryl monostearate (180 mg) in CH_2Cl_2 (20 mL) under a constant stirring at 400 rpm. The aqueous phase was created by dissolving poloxamer 188 in pure water at 50°C. The oil phase was added dropwise to the aqueous phase and the organic solvent removed at 50°C under vacuum using a rotary evaporator. Then, the mixture was ultrasonically dispersed at 50°C and cooled to room temperature to obtain EtpP–CDDP NLCs (Figure 2).

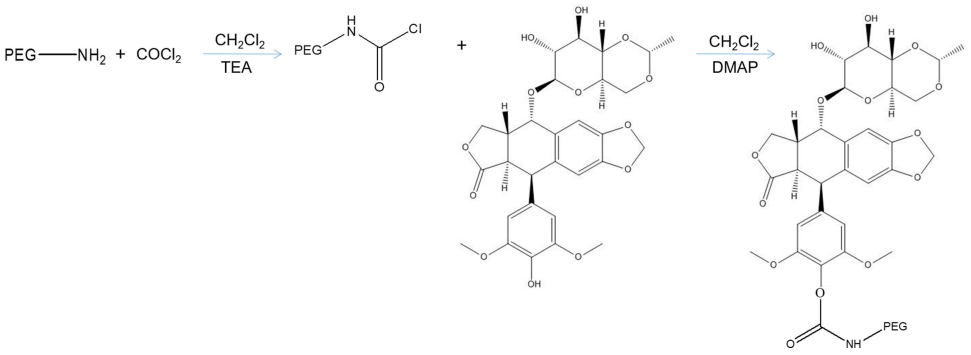

Figure 1 The Etp prodrug was synthesized by linking the phenolic hydroxyl group of Etp with PEG.
Note: ETP prodrug was synthesized by linking the phenolic hydroxyl group of ETP with PEG.

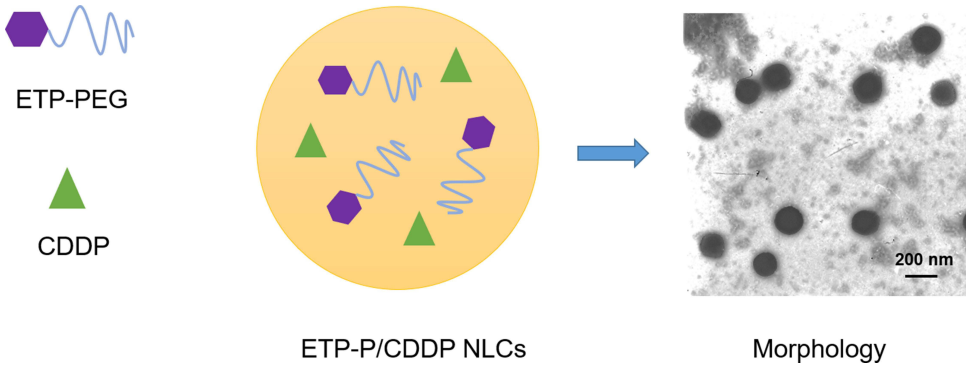

Figure 2 EtpP–CDDP NLCs and TEM. EtpP–CDDP NLCs were prepared using film ultrasound. The morphology of EtpP–CDDP NLCs was examined using transmission electron microscopy (TEM).
Note: ETP-P/CDDP NLCs were prepared using film-ultrasonic method.

Etp (not prodrug) and CDDP coloaded NLCs (Etp–CDDP NLCs) were prepared by the same method using Etp and PEG (20 mg) instead of EtpP (20 mg). EtpP- or CDDP-loaded NLCs (EtpP NLCs or CDDP NLCs) were prepared by the same method using Etp (20 mg) or CDDP (10 mg), without adding another drug. Blank NLCs were prepared by the same method using no drug.

Particle Size, ζ-Potential, and Stability

Particle sizes, polydispersity index (PDI) values, and ζ-potential of NLCs were determined using a laser light scattering.[24] Morphology of EtpP–CDDP NLCs was examined using transmission electron microscopy. A drop of EtpP–CDDP NLC suspension was placed on a copper grid and air-dried, followed by negative staining with one drop of 3% aqueous solution of sodium phosphotungstate. Photos were taken after air-drying. The stability of NLCs was checked in PBS at 2°C–8°C and cell-culture medium (DMEM + 10% FBS) at 37°C. Changes in particle size and appearance were recorded over time.

Drug Loading and In Vitro Drug Release

Drug-encapsulation efficiency (EE) and -loading capacity (LC) of NLCs were detected by separating the drugs from NLCs under centrifugation (10,000 rpm for 10 min). The amount of loaded drugs in NLCs was determined by UV–visible spectroscopy using a UV spectrophotometer.[25] The selected wavelengths used for the measurement of Etp and CDDP were 254 nm and 210 nm, respectively.[9,25] EE and LC were calculated by:

EE (%) = amount of entrapped drugs/total weight of drugs × 100.

LC (%) = amount of drugs in nanoparticles/mass of nanoparticles × 100.

In vitro release of drugs from NLCs was analysed using dialysis at 37°C.[26,27] In brief, NLCs (2 mL) were put into a dialysis bag and immersed in 100 mL PBS in the presence of 10% FBS (pH 7.4) and placed on a shaking bed at 37°C with a rotation speed of 100 rpm. Samples (2 mL) were withdrawn at predetermined time intervals and replaced by 2 mL fresh release medium. The released drugs were analyzed by the same method as previously mentioned.

Cellular Uptake

Cellular uptake of NLCs was visualized using an inversion fluorescence microscope (CKX53; Olympus, Tokyo, Japan) and quantified by fluorescence-activated cell sorting.[28] C_6 was used as the fluorescent probe and C_6-containing NLCs were prepared by the same method, adding C_6 (5 mg) along with doxorubicin in the oil phase. A549/DDP cells were seeded in 24-well culture plates (5×10^4 cells per well) and incubated with various formulations (200 μg/mL) for 2 h. After incubation, cells were washed three times with D-Hank's solution, photographed with the inversion fluorescence microscope, and quantified using a fluorescence-activated cell sorter (FACS, Becton, Dickinson, Franklin Lakes, NJ, $\lambda_{excitation}$ 430 nm, $\lambda_{emission}$ 485 nm).

Cytotoxicity and Synergistic Effect

Cytotoxicity of drugs and drug-containing NLCs was assessed by evaluating cell viability using MTT assays.[29] A549/DDP cells, BEAS-2B, cells or HUVECs (2×10^4 cells/well) were seeded in 96-well plates and allowed to grow for 24 h, then were treated with EtpP–CDDP NLCs, Etp–CDDP NLCs, EtpP NLCs, CDDP NLCs, blank NLCs, free EtpP–CDDP, free EtpP, and free CDDP at various drug concentrations. After 48 h of incubation, the medium in each well was replaced with fresh medium (100 μL), 10 μL MTT solution (5 mg/mL) added to each well (10% v/v), and cells further incubated for 4 hours at 37°C. DMSO (150 μL) was added to each well after the removal of medium and shaken for 10 minutes. A microplate reader was utilized to record absorbance at a wavelength of 570 nm. Mean drug concentration required for 50% growth inhibition (IC_{50}) was calculated.

An effective method to evaluate synergistic drug combinations in vitro is median-effect analysis, introduced by Chou and Talalay.[30] The median-effect method assesses drug–drug interaction using a "combination index" (CI), which is based on the concentration–response relationship.[31] CI < 1 represents synergism and CI > 1 represents antagonism. In this study, values were calculated by CI_{50} = (concentration of Etp in combination system)/(IC_{50} of Etp) + (concentration of CDDP in combination system)/(IC_{50} of CDDP). Caspase 3 activity assays were carried out according to the instructions of the manufacturer with a caspase 3 activity kit (Beyotime, Shanghai, China).[32,33] After treatment with EtpP–CDDP NLCs, Etp–CDDP NLCs, EtpP NLCs, CDDP NLCs, blank NLCs, free EtpP–CDDP, free EtpP, and free CDDP (100 μg/mL for 24 h), A549/DDP cells were washed, collected, lysed, centrifuged, and analyzed for total protein by a SpectraMax M2 microplate reader (Molecular Devices, USA) at 405 nm.

In Vivo Pharmacokinetics and Tissue Distribution

BALB/c nude mice were injected with A549/DDP cells in the right flank to produce lung cancer–bearing xenografts. When tumors had grown to a volume of about 100 mm^3, the mice were randomly divided into three groups (six in each group). EtpP–CDDP NLCs, Etp–CDDP NLCs, and free EtpP–CDDP were intravenously injected in mice at a drug dose of 5 mg/kg body weight.[34,35] At determined time points, blood (500 μL) was collected by cardiac puncture after euthanizing the mice. Plasma was separated by centrifuging samples (2500 rpm, 15 min). At 1 h and 48 h, the tumor tissue and other main tissue types (heart, liver, spleen, lung, and kidney) were removed, washed, and homogenized. The mixture was vortexed and centrifuged (15,000 rpm, 10 min), and the supernatants along with the plasma concentration of drugs were determined by the same method as in the Drug Loading and In Vitro Drug Release section.

In Vivo Toxicity and Antitumor Ability

Lung cancer–bearing xenografts were randomly divided into nine groups (six in each group). EtpP–CDDP NLCs, Etp–CDDP NLCs, EtpP NLCs, CDDP NLCs, blank NLCs, free EtpP–CDDP, free EtpP, free CDDP, and 0.9% saline were intravenously injected in the tail vein every 3 days.[36] The sizes of the tumors were measured using calipers before every injection, and tumor volume was calculated by long axis × (short axis)^2/2. In vivo toxicity was observed by monitoring

changes in the body weights of mice every 3 days and white blood cells (WBCs), alanine aminotransferase (Alt; liver function), and creatinine (Cre; kidney function).

Statistical Analysis

The sample size in all experiments was at least six (n≥6). Data distribution was assessed with Shapiro–Wilk tests and QQ plots. Statistical analysis was performed using unpaired *t*-tests (between two groups) and one-way ANOVA (among three or more groups), followed by Tukey's post hoc test using SPSS 20.0. Statistical significance was taken as $P<0.05$. Data are presented as means ± SD.

Results

Characterization of EtpP–CDDP NLCs

EtpP–CDDP NLCs showed a uniformly spherical morphology (Figure 2) with a size of 176.8±4.9 nm and ζ-potential of –31.9±3.2 mV (Table 1). The EE of NLCs was around 90% and that of LCs 3.3%–5.4%. The stability of NLCs was evaluated by changes in size, presented in Figure 3. NLC formulations showed good stability during 90 days of storage in PBS at 2°C–8°C, while NLCs remained stable in the first 6 days (Figure 4). In vitro drug release of both EtpP and CDDP from LPNs was sustained. The drugs had completed their release from NLCs by 48 h, which could be a reference for in vitro and in vivo antitumor studies.

Cellular Uptake

Figure 5 illustrate the cellular uptake efficiency of EtpP–CDDP NLCs, Etp–CDDP NLCs and blank NLCs: 57.4%±3.9%, 55.1%±4.1% and 59.2%±3.5% into A549/DDP cells, respectively. This could be recognized as high cellular uptake of the carriers, as illustrated by Hong et al and Pang et al[28,37]

Cytotoxicity and Synergistic Effect

Blank NLCs did not change cell viability, while free drug and drug-loaded NLCs showed obvious cell-inhibition efficiency compared with the control ($P<0.05$) EtpP–CDDP NLCs exhibited higher cytotoxicity than Etp–CDDP NLCs, EtpP NLCs, and free EtpP–CDDP on A549/DDP cells (Figure 6A and Supplementary Figure 1, $P<0.05$). On the contrary, drug-loaded NLCs did not exhibit enhanced cell inhibition on human normal lung epithelial cells (BEAS-2B cells) or HUVECs compared with free drugs (Figure 6B and C). The CI_{50} values that illustrated the synergistic effect of the dual drug–containing systems are presented in Figure 6D, which shows that CI values were <1 with fraction of affected cells (Fa) of 20%–80% (0.2–0.8). Caspase 3 activity assays showed that caspase activity in A549/DDP cells treated with EtpP–CDDP NLCs increased significantly in comparison to Etp–CDDP NLCs, EtpP NLCs, and free EtpP–CDDP ($P<0.05$). This indicated that EtpP–CDDP NLCs promoted caspase 3 activation in lung cancer cells (Figure 6E).

Table 1 Characterization of NLCs (means ± SD, n=8)

	EtpP–CDDP NLCs	Etp–CDDP NLCs	EtpP NLCs	CDDP NLCs	Blank NLCs
Particle size (nm)	176.8±4.9	172.3±4.5	169.9±5.1	170.8±4.8	168.5±4.3
PDI	0.15±0.02	0.14±0.02	0.17±0.03	0.13±0.02	0.12±0.01
ζ-potential (mV)	–31.9±3.2	–33.4±2.9	–29.7±3.1	–30.6±2.7	–28.9±3.3
EE of Etp (%)	88.9±3.4	86.7±3.1	85.8±3.3	/	/
EE of CDDP (%)	90.2±2.1	91.3±1.9	/	92.1±2.2	/
LC of Etp (%)	5.1±0.5	5.4±0.6	4.9±0.4	/	/
LC of CDDP (%)	3.3±0.4	3.5±0.3	/	3.6±0.5	/

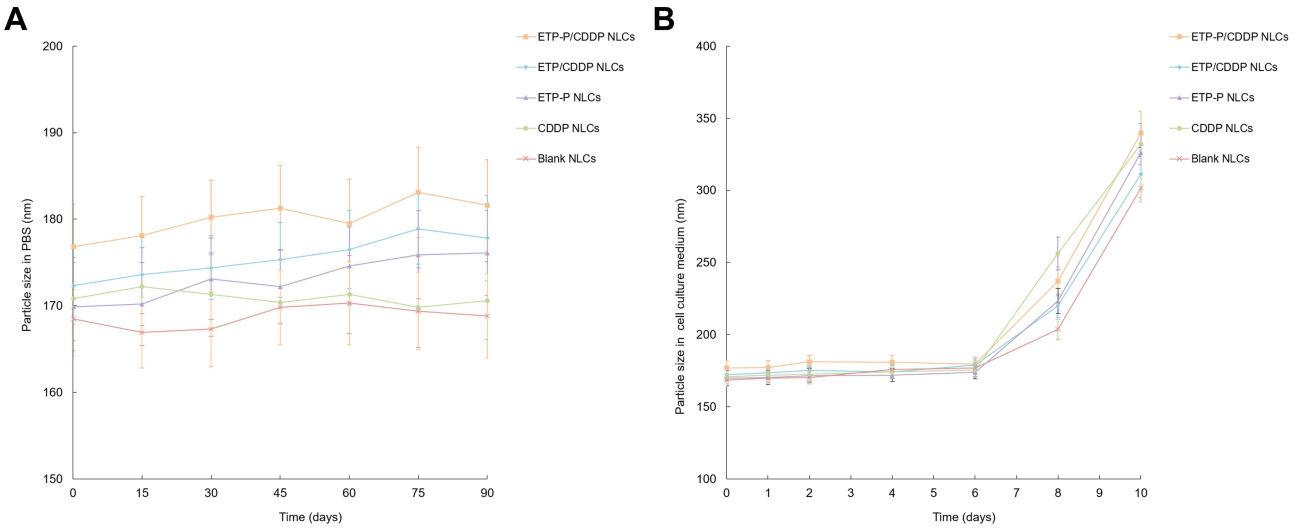

Figure 3 The stability of NLCs evaluated in PBS at 2°C–8°C (**A**) and cell-culture medium (DMEM + 10% FBS) at 37°C (**B**) by changes in size with time.
Note: Data presented as means ± SD, n=6.

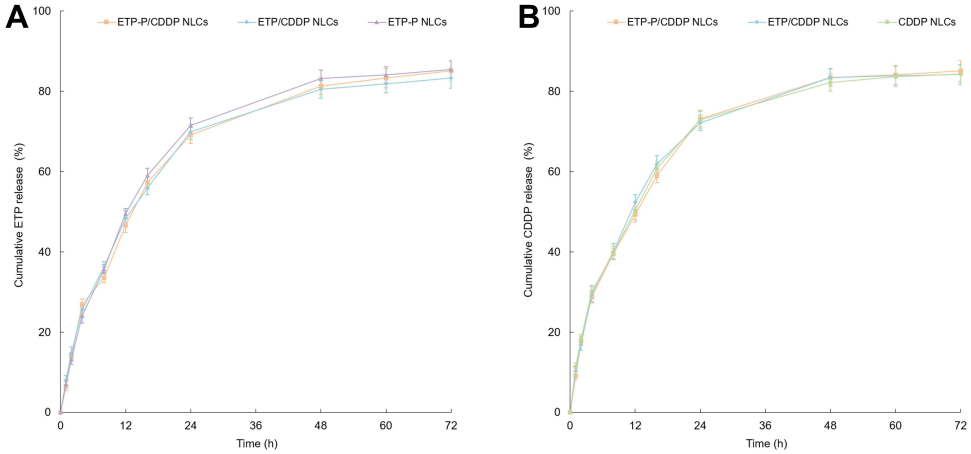

Figure 4 In vitro release of Etp (**A**) and CDDP (**B**) from NLCs was analyzed using dialysis. NLCs (2 mL) were put in a dialysis bag, immersed in 100 mL PBS in the presence of 10% FBS (pH 7.4), and placed on a shaking bed at 37°C with a rotation speed of 100 rpm.
Note: Data presented as means ± SD, n=6.

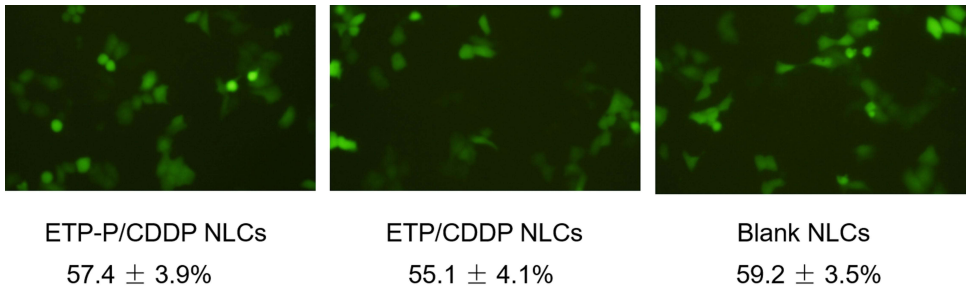

Figure 5 Cellular uptake efficiency of EtpP–CDDP NLCs, Etpp–CDDP NLCs, and blank NLCs. Uptake of NLCs was visualized using inversion fluorescence microscopy and quantified by fluorescence-activated cell sorting.
Note: Data presented as means ± SD, n=6.

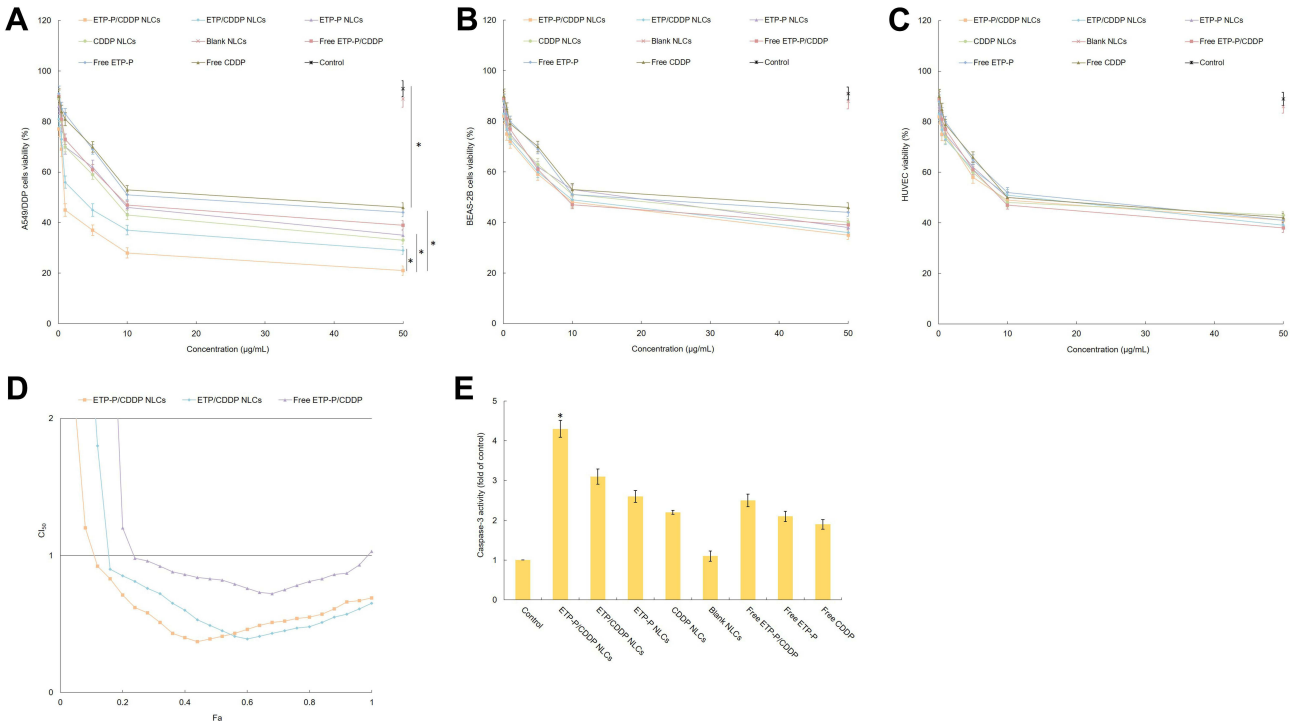

Figure 6 Cytotoxicity of drugs and drug-containing NLCs assessed by evaluating A549/DDP (**A**), BEAS-2B (**B**), and HUVECs (**C**) viability using MTT assays. A549/DDP and BEAS-2B cells (2×10^4 cells/well) were seeded in 96-well plates and allowed to grow for 24 h, then were treated with EtpP–CDDP NLCs, Etpp–CDDP NLCs, EtpP NLCs, CDDP NLCs, blank NLCs, free EtpP–CDDP, free EtpP, and free CDDP at various drug concentrations. CI_{50} values illustrated the synergistic effect of the dual drug–containing systems (**D**). Caspase 3 activity assays were carried out according to the instructions of the manufacturer with a caspase 3 activity kit (**E**). *P<0.05.
Note: Data presented as means ± SD, n=6.

In Vivo Pharmacokinetics and Tissue Distribution

The blood concentration–time profiles of EtpP–CDDP NLCs, Etp–CDDP NLCs, and free EtpP–CDDP are presented in Figure 7. EtpP–CDDP NLCs and Etp–CDDP NLCs exhibited more sustained plasma retention effects than the rapidly decreasing concentration of free EtpP–CDDP. Tissue biodistribution of drugs is summarized in Figure 8. At both 1 and 48 h after intravenous injection, EtpP–CDDP NLCs showed higher drug distribution in tumors than Etp–CDDP NLCs and free EtpP–CDDP (Supplementary Figures 2 and 3, P<0.05). Etp–CDDP NLCs exhibited higher tumor drug accumulation than free EtpP–CDDP (P<0.05). Tumor accumulation of free EtpP–CDDP decreased rapidly after 48 h, while NLC formulations remained at high levels at 48 h.

In Vivo Antitumor Ability

In vivo antitumor ability of drug-loaded NLCs and free drugs were investigated on lung cancer–bearing mice (Figure 9). Drug-loaded NLC groups showed remarkably higher tumor inhibition compared to free drugs (Figure 9A and Supplementary Figure 4, P<0.05). Dual drug–loaded EtpP–CDDP NLCs exhibited higher inhibit rates than single drug–loaded NLCs (P<0.05). Most importantly, EtpP–CDDP NLCs illustrated enhanced antitumor efficacy than non-prodrug–containing Etp–CDDP NLCs (P<0.05). Figure 9B shows that drug-containing NLCs did not cause changes in body weight, while free drugs caused a decrease in weight (Supplementary Figure 5, P<0.05). An increase in Cre was observed in the free-drug groups (Figure 9C), while the Alt and WBC values of NLCs and free drugs were not obviously changed (Figure 9A and B).

Discussion

At the beginning of this study, an Etp prodrug was synthesized. Under controlled conditions (DMAP and CH_2Cl_2), the alcohol groups of the Etp glucose moiety did not react, and only the –OH phenol group was coupled with Etp.[26] After that, dual drug–loaded NLCs were prepared. NLCs have been reported to be nanosized with narrow size distribution and

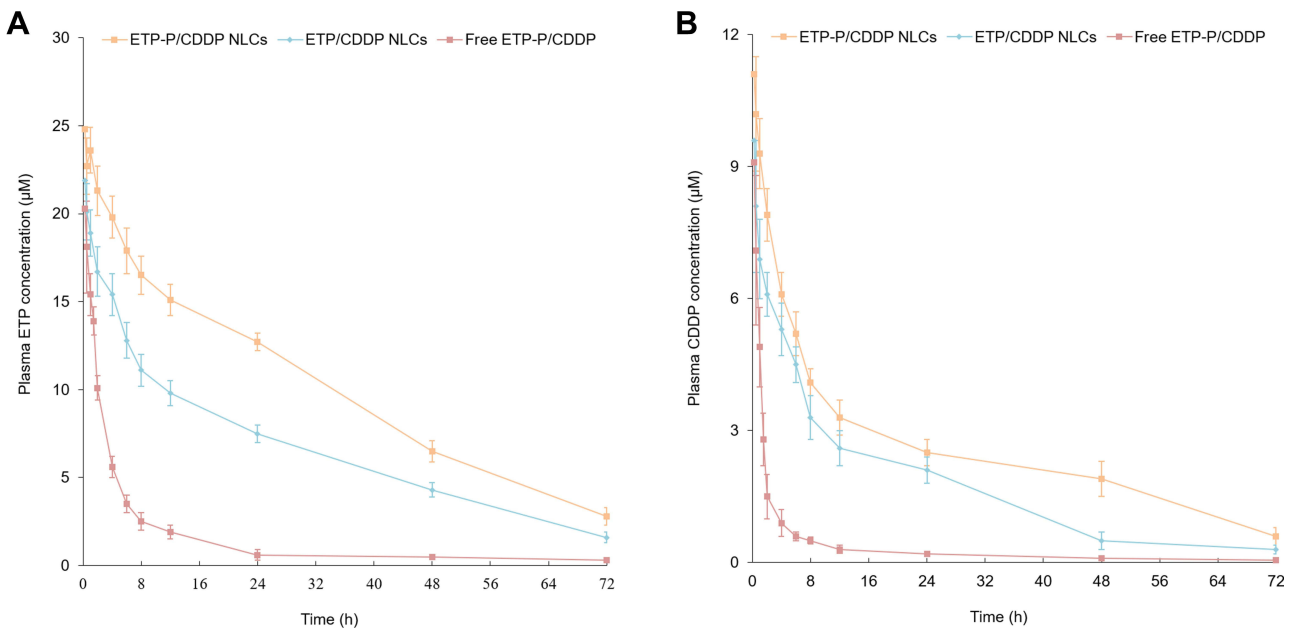

Figure 7 Etp (**A**) and CDDP (**B**) blood concentration–time profiles of EtpP–CDDP NLCs, Etpp–CDDP NLCs, and free EtpP–CDDP. Mixtures were vortexed and centrifuged (15,000 rpm, 10 min), and supernatants and plasma concentration of drugs were determined.
Note: Data presented as means ± SD, n=6.

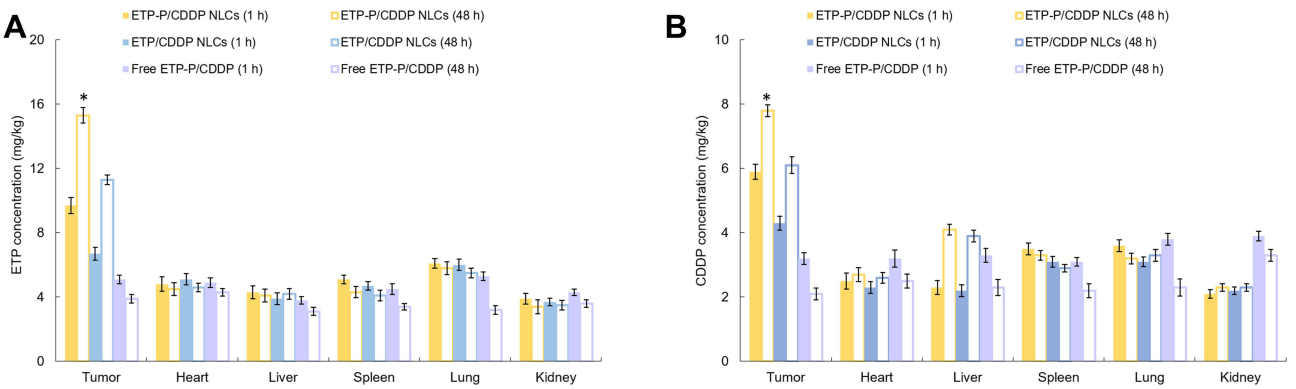

Figure 8 Tissue Etp (**A**) and CDDP (**B**) biodistribution of EtpP–CDDP NLCs, Etpp–CDDP NLCs, and free EtpP–CDDP. At 1 and 48 h, the tumor tissue and other main tissue types (heart, liver, spleen, lung, and kidney) were removed, washed, homogenized, and analyzed. *$P<0.05$.
Note: Data presented as means ± SD, n=6.

high drug EE.[38] The size of the prepared NLCs was around 170 nm, which proved to be efficiently internalized into cells.[39] The EE of NLCs was about 90%, which promised good loading ability of the systems.[40]

The release profiles of the NLCs revealed a two-stage process, with relatively fast drug release in the initial stage and slow release subsequently, which was also described by Luan et al.[41] The biphasic drug-release patterns in that study were described as fast release in the initial 12 h, about 50%, followed by sustained release 30% of the remaining by 48 h. This phenomenon was caused by the drug concentration gradient between the nanoparticle and the medium: a burst release of the drug dispersed on the surface of NLCs in the initial stage, then gradual release due to the amount of drug in the nanoparticles depleting with the release process.[41] Cellular uptake of nanoparticles can be quantitatively detected by the fluorescence method.[39] Cellular uptake efficiency of NLCs was >50%, which may be recognized as relatively high.[33,37]

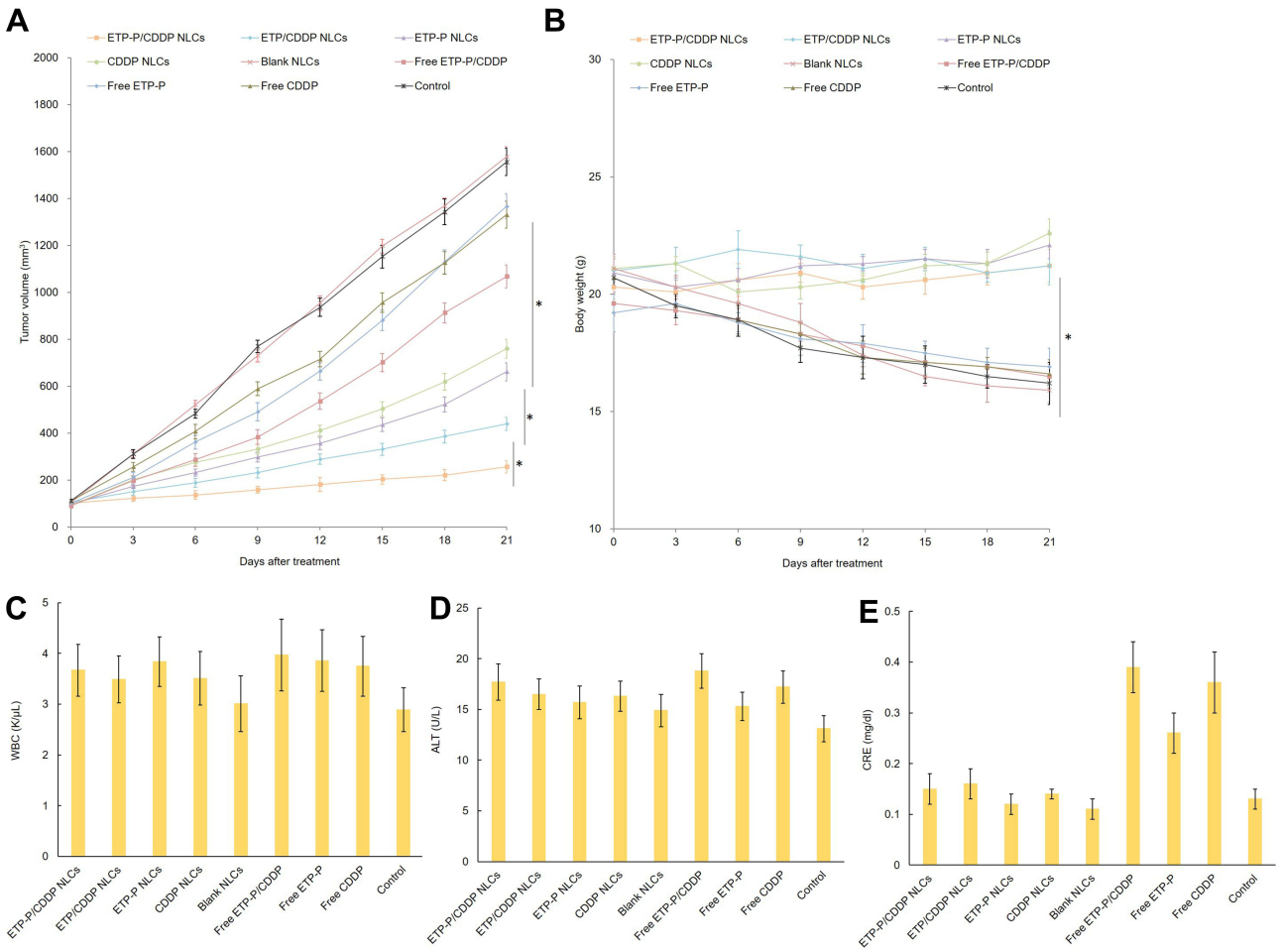

Figure 9 In vivo antitumor activity (**A**), body-weight changes (**B**), WBC (**C**), Alt (**D**), and Cre (**E**) in lung cancer–bearing mice. Tumor sizes were measured using calipers before every injection and tumor volume calculated by long axis × (short axis)^2/2. Body-weight changes were monitored every 3 days to evaluate systemic toxicity. *P<0.05.
Note: Data presented as means ± SD, n=6.

Nanoparticulate drug-delivery systems may induce significant cytotoxic effects in systems, because free drugs diffuse through cell membranes, but nanoparticles are internalized through the endocytic pathway, resulting in greater uptake and higher cytotoxicity than free drugs.[42] EtpP–CDDP NLCs exhibited higher cytotoxicity than Etp–CDDP NLCs, EtpP NLCs and free EtpP–CDDP on A549/DDP cells. This may prove the enhanced ability of the NLCs, which were able to adhere to the cell membrane due to the similar nature of the lipids and the cell membrane.[43] This characteristic may enhance intracellular drug accumulation and perform better in cancer therapy. Combination therapy using nanoparticles containing CDDP has received much interest in cancer therapy to overcome CDDP-resistan, eg, Liang et al developed a CDDP and vinorelbine coencapsulated nano-platform for lung cancer treatment.[44] When combination therapy is used in the system, evaluation of the synergistic effect is important, and CI analyses are one of the most reliable methods.[45] The CI_{50} values of the systems tested in this research were <1, which illustrated the synergistic effect of the dual drug–containing systems.

In vivo pharmacokinetic and tissue-distribution studies were carried out on lung cancer–bearing mice. Higher accumulation in tumor tissue may contribute to the passive targeting ability of nanoparticles through the enhanced permeability-and-retention (EPR) effect.[46] In vivo tumor-inhibition results showed that blank NLCs had similar tumor-growth curves as controls, suggesting that nanomaterials without drug could not inhibit tumor growth.[19] EtpP–CDDP NLCs showed the most significant antitumor efficiency (P=0.0186), better than non-prodrug–containing Etp–CDDP NLCs. This result is in accordance with the findings of Wang et al that prodrug-based systems can improve lung cancer chemotherapy.[47] Mice treated with nanoparticles showed negligible changes in Cre, Alt, and WBCs over the control group, while free drugs affected some parameters. No obvious weight loss was observed in any of the test NLC groups,

indicating good tolerance of the systems, which was also reported by Zhang et al, ie, the lipid structure of NLCs has high affinity with the lipid cell surface, promotes the fusion of carriers to cells, and thus delivers the drug without high systemic toxicity.[48]

Conclusion

An Etp prodrug was synthesized and EtpP–CDDP NLCs prepared. EtpP–CDDP NLCs exhibited high tumor-cell uptake, high cytotoxicity, sustained plasma retention effect, increased accumulation in tumor tissue, and improved tumor-inhibition efficiency. These characteristics could make this a promising drug-delivery system for lung cancer combination therapy.

Disclosure

The authors report no conflicts of interest in relation to this work.

References

1. Torre LA, Siegel RL, Jemal A. Lung cancer statistics. *Adv Exp Med Biol*. 2016;893:1–19.
2. Ettinger DS, Wood DE, Aisner DL, et al. Non-small cell lung cancer, version 5.2017, NCCN clinical practice guidelines in oncology. *J Natl Compr Canc Netw*. 2017;15(4):504–535. doi:10.6004/jnccn.2017.0050
3. Mottaghitalab F, Farokhi M, Fatahi Y, Atyabi F, Dinarvand R. New insights into designing hybrid nanoparticles for lung cancer: diagnosis and treatment. *J Control Release*. 2019;295:250–267. doi:10.1016/j.jconrel.2019.01.009
4. Howlader N, Noone AM, Krapcho M, et al. *SEER Cancer Statistics Review, 1975–2016, Based on November 2018 SEER Data Submission, Posted to the SEER Web Site, April 2019*. Bethesda, MD: National Cancer Institute; 2019.
5. Arriagada R, Bergman B, Dunant A, Le Chevalier T, Pignon JP, Vansteenkiste J; International Adjuvant Lung Cancer Trial Collaborative Group. Cisplatin-based adjuvant chemotherapy in patients with completely resected non-small-cell lung cancer. *N Engl J Med*. 2004;350(4):351–360.
6. Winton T, Livingston R, Johnson D, et al.; National Cancer Institute of Canada Clinical Trials Group; National Cancer Institute of the United States Intergroup JBR.10 Trial Investigators. Vinorelbine plus cisplatin vs. observation in resected non-small-cell lung cancer. *N Engl J Med*. 2005;352(25):2589–2597. doi:10.1056/NEJMoa043623
7. Senan S, Brade A, Wang LH, et al. PROCLAIM: randomized Phase III trial of pemetrexed-cisplatin or etoposide-cisplatin plus thoracic radiation therapy followed by consolidation chemotherapy in locally advanced nonsquamous non-small-cell lung cancer. *J Clin Oncol*. 2016;34(9):953–962. doi:10.1200/JCO.2015.64.8824
8. Mymryk JS, Zaniewski E, Archer TK. Cisplatin inhibits chromatin remodeling, transcription factor binding, and transcription from the mouse mammary tumor virus promoter in vivo. *Proc Natl Acad Sci U S A*. 1995;92(6):2076–2080. doi:10.1073/pnas.92.6.2076
9. Khan MM, Madni A, Tahir N, et al. Co-Delivery of Curcumin and Cisplatin to Enhance Cytotoxicity of Cisplatin Using Lipid-Chitosan Hybrid Nanoparticles. *Int J Nanomedicine*. 2020;15:2207–2217. doi:10.2147/IJN.S247893
10. Zhu LJ, Gu LS, Shi TY, Zhang XY, Sun BW. Enhanced treatment effect of nanoparticles containing cisplatin and a GSH-reactive probe compound. *Mater Sci Eng C Mater Biol Appl*. 2019;96:635–641. doi:10.1016/j.msec.2018.11.039
11. Hande KR. Etoposide: four decades of development of a topoisomerase II inhibitor. *Eur J Cancer*. 1998;34(10):1514–1521. doi:10.1016/S0959-8049(98)00228-7
12. Yordanov G, Skrobanska R, Evangelatov A. Colloidal formulations of etoposide based on poly(butyl cyanoacrylate) nanoparticles: preparation, physicochemical properties and cytotoxicity. *Colloids Surf B Biointerfaces*. 2013;101:215–222. doi:10.1016/j.colsurfb.2012.05.040
13. Jornada DH, Dos Santos Fernandes GF, Chiba DE, de Melo TR, Dos Santos JL, Chung MC. The prodrug approach: a successful tool for improving drug solubility. *Molecules*. 2015;21(1):42. doi:10.3390/molecules21010042
14. Rautio J, Kumpulainen H, Heimbach T, et al. Prodrugs: design and clinical applications. *Nat Rev Drug Discov*. 2008;7(3):255–270. doi:10.1038/nrd2468
15. Schmidt F, Monneret C. Prodrug Mono Therapy: synthesis and biological evaluation of an etoposide glucuronide-prodrug. *Bioorg Med Chem*. 2003;11(10):2277–2283. doi:10.1016/S0968-0896(03)00108-1
16. Medical Advisory Secretariat. Nanotechnology: an evidence-based analysis. *Ont Health Technol Assess Ser*. 2006;6(19):1–43.
17. De Jong WH, Borm PJ. Drug delivery and nanoparticles: applications and hazards. *Int J Nanomedicine*. 2008;3(2):133–149. doi:10.2147/IJN.S596
18. Chen G, Zhang Y, Deng H, Tang Z, Mao J, Wang L. Pursuing for the better lung cancer therapy effect: comparison of two different kinds of hyaluronic acid and nitroimidazole co-decorated nanomedicines. *Biomed Pharmacother*. 2020;125:109988. doi:10.1016/j.biopha.2020.109988
19. Cao C, Wang Q, Liu Y. Lung cancer combination therapy: doxorubicin and β-elemene co-loaded, pH-sensitive nanostructured lipid carriers. *Drug Des Devel Ther*. 2019;13:1087–1098. doi:10.2147/DDDT.S198003
20. Guo S, Zhang Y, Wu Z, et al. Synergistic combination therapy of lung cancer: cetuximab functionalized nanostructured lipid carriers for the co-delivery of paclitaxel and 5-Demethylnobiletin. *Biomed Pharmacother*. 2019;118:109225. doi:10.1016/j.biopha.2019.109225
21. Rawal S, Patel B, Patel MM. Fabrication, optimisation and in vitro evaluation of docetaxel and curcumin Co-loaded nanostructured lipid carriers for improved antitumor activity against non-small cell lung carcinoma. *J Microencapsul*. 2020;37(8):543–556. doi:10.1080/02652048.2020.1823498
22. Shabat D, Lode HN, Pertl U, et al. In vivo activity in a catalytic antibody-prodrug system: antibody catalyzed etoposide prodrug activation for selective chemotherapy. *Proc Natl Acad Sci U S A*. 2001;98(13):7528–7533. doi:10.1073/pnas.131187998
23. Zhang K, Lv S, Li X, et al. Preparation, characterization, and in vivo pharmacokinetics of nanostructured lipid carriers loaded with oleanolic acid and gentiopicrin. *Int J Nanomedicine*. 2013;8:3227–3239. doi:10.2147/IJN.S45031
24. Hong Y, Che S, Hui B, et al. Lung cancer therapy using doxorubicin and curcumin combination: targeted prodrug based, pH sensitive nanomedicine. *Biomed Pharmacother*. 2019;112:108614. doi:10.1016/j.biopha.2019.108614
25. Zhu R, Wang Q, Zhu Y, et al. pH sensitive nano layered double hydroxides reduce the hematotoxicity and enhance the anticancer efficacy of etoposide on non-small cell lung cancer. *Acta Biomater*. 2016;29:320–332. doi:10.1016/j.actbio.2015.10.029

26. Song Z, Shi Y, Han Q, Dai G. Endothelial growth factor receptor-targeted and reactive oxygen species-responsive lung cancer therapy by docetaxel and resveratrol encapsulated lipid-polymer hybrid nanoparticles. *Biomed Pharmacother*. 2018;105:18–26. doi:10.1016/j.biopha.2018.05.095
27. Xu G, Chen Y, Shan R, Wu X, Chen L. Transferrin and tocopheryl-polyethylene glycol-succinate dual ligands decorated, cisplatin loaded nano-sized system for the treatment of lung cancer. *Biomed Pharmacother*. 2018;99:354–362. doi:10.1016/j.biopha.2018.01.062
28. Zheng G, Zheng M, Yang B, Fu H, Li Y. Improving breast cancer therapy using doxorubicin loaded solid lipid nanoparticles: synthesis of a novel arginine-glycine-aspartic tripeptide conjugated, pH sensitive lipid and evaluation of the nanomedicine in vitro and in vivo. *Biomed Pharmacother*. 2019;116:109006. doi:10.1016/j.biopha.2019.109006
29. Wang G, Wang Z, Li C, et al. RGD peptide-modified, paclitaxel prodrug-based, dual-drugs loaded, and redox-sensitive lipid-polymer nanoparticles for the enhanced lung cancer therapy. *Biomed Pharmacother*. 2018;106:275–284. doi:10.1016/j.biopha.2018.06.137
30. Chou TC. Theoretical basis, experimental design, and computerized simulation of synergism and antagonism in drug combination studies. *Pharmacol Rev*. 2006;58:621e81. doi:10.1124/pr.58.3.10
31. Cai L, Xu G, Shi C, Guo D, Wang X, Luo J. Telodendrimer nanocarrier for co-delivery of paclitaxel and cisplatin: a synergistic combination nanotherapy for ovarian cancer treatment. *Biomaterials*. 2015;37:456–468. doi:10.1016/j.biomaterials.2014.10.044
32. Baharara J, Ramezani T, Divsalar A, Mousavi M, Seyedarabi A. Induction of apoptosis by green synthesized gold nanoparticles through activation of caspase-3 and 9 in human cervical cancer cells. *Avicenna J Med Biotechnol*. 2016;8(2):75–83.
33. Wang P, Wang H, Huang Q, et al. Exosomes from M1-polarized macrophages enhance paclitaxel antitumor activity by activating macrophages-mediated inflammation. *Theranostics*. 2019;9(6):1714–1727. doi:10.7150/thno.30716
34. Thomas AM, Kapanen AI, Hare JI, et al. Development of a liposomal nanoparticle formulation of 5-fluorouracil for parenteral administration: formulation design, pharmacokinetics and efficacy. *J Control Release*. 2011;150(2):212–219. doi:10.1016/j.jconrel.2010.11.018
35. Sun G, Sun K, Sun J. Combination prostate cancer therapy: prostate-specific membranes antigen targeted, pH-sensitive nanoparticles loaded with doxorubicin and tanshinone. *Drug Deliv*. 2021;28(1):1132–1140. doi:10.1080/10717544.2021.1931559
36. Shao Y, Luo W, Guo Q, Li X, Zhang Q, Li J. In vitro and in vivo effect of hyaluronic acid modified, doxorubicin and gallic acid co-delivered lipid-polymeric hybrid nano-system for leukemia therapy. *Drug Des Devel Ther*. 2019;13:2043–2055. doi:10.2147/DDDT.S202818
37. Hong Y, Che S, Hui B, Wang X, Zhang X, Ma H. Combination therapy of lung cancer using layer-by-layer cisplatin prodrug and curcumin co-encapsulated nanomedicine. *Drug Des Devel Ther*. 2020;14:2263–2274. doi:10.2147/DDDT.S241291
38. Jiang H, Geng D, Liu H, Li Z, Cao J. Co-delivery of etoposide and curcumin by lipid nanoparticulate drug delivery system for the treatment of gastric tumors. *Drug Deliv*. 2016;23(9):3665–3673. doi:10.1080/10717544.2016.1217954
39. Wang J. Combination treatment of cervical cancer using folate-decorated, pH-sensitive, carboplatin and paclitaxel co-loaded lipid-polymer hybrid nanoparticles. *Drug Des Devel Ther*. 2020;14:823–832. doi:10.2147/DDDT.S235098
40. Macedo LB, Nogueira-Librelotto DR, de Vargas J, Scheeren LE, Vinardell MP, Rolim CMB. Poly (ε-Caprolactone) nanoparticles with pH-responsive behavior improved the in vitro antitumor activity of methotrexate. *AAPS Pharm Sci Tech*. 2019;20(5):165. doi:10.1208/s12249-019-1372-5
41. Luan J, Zhang D, Hao L, et al. Preparation, characterization and pharmacokinetics of Amoitone B-loaded long circulating nanostructured lipid carriers. *Colloids Surf B Biointerfaces*. 2014;114:255–260. doi:10.1016/j.colsurfb.2013.10.018
42. Mao K, Zhang W, Yu L, Yu Y, Liu H, Zhang X. Transferrin-decorated protein-lipid hybrid nanoparticle efficiently delivers cisplatin and docetaxel for targeted lung cancer treatment. *Drug Des Devel Ther*. 2021;15:3475–3486. doi:10.2147/DDDT.S296253
43. Chen W, Guo M, Wang S. Anti prostate cancer using PEGylated bombesin containing, cabazitaxel loading nano-sized drug delivery system. *Drug Dev Ind Pharm*. 2016;42(12):1968–1976. doi:10.1080/03639045.2016.1185438
44. Bao H, Zheng N, Li Z, Zhi Y. Synergistic effect of tangeretin and atorvastatin for colon cancer combination therapy: targeted delivery of these dual drugs using RGD peptide decorated nanocarriers. *Drug Des Devel Ther*. 2020;14:3057–3068. doi:10.2147/DDDT.S256636
45. Liang Z, Li J, Zhu B. Lung cancer combination treatment: evaluation of the synergistic effect of cisplatin prodrug, vinorelbine and retinoic acid when co-encapsulated in a multi-layered nano-platform. *Drug Des Devel Ther*. 2020;14:4519–4531. doi:10.2147/DDDT.S251749
46. Tan S, Wang G. Redox-responsive and pH-sensitive nanoparticles enhanced stability and anticancer ability of erlotinib to treat lung cancer in vivo. *Drug Des Devel Ther*. 2017;11:3519–3529. doi:10.2147/DDDT.S151422
47. Wang B, Hu W, Yan H, et al. Lung cancer chemotherapy using nanoparticles: enhanced target ability of redox-responsive and pH-sensitive cisplatin prodrug and paclitaxel. *Biomed Pharmacother*. 2021;136:111249. doi:10.1016/j.biopha.2021.111249
48. Zhang J, Xiao X, Zhu J, et al. Lactoferrin- and RGD-comodified, temozolomide and vincristine-coloaded nanostructured lipid carriers for gliomatosis cerebri combination therapy. *Int J Nanomedicine*. 2018;13:3039–3051. doi:10.2147/IJN.S161163